On the Fluorescence Depolarization and the Calculation of Rotational Relaxation Times of Rigid Rod Molecules

E. Birckner[1,2] and U.-W. Grummt[1]

The rotational relaxation times of rod like molecules like poly[arylene-ethynylene]s and their low molecular weight model compounds calculated from a simple model agree well with the experimental ones as long as the axial ratio of the corresponding rotational ellipsoid is less than 8. For the polymer (axial ratio >10) the fluorescence depolarization cannot be described by rotational motion perpendicularly to the long molecular axis. One has to take into consideration bending motions in connection with energy transfer along the bent backbone.
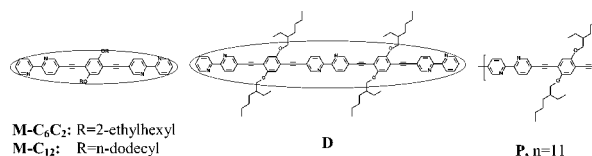
INTRODUCTION

Fluorescence depolarization originates from different spatial orientations of the absorption and the emission transition moments. In the case of identical absorbing and emitting states ($S_0 \leftrightarrow S_1$) the dynamics of the depolarization of non fixed molecules is essentially governed by rotational diffusion. It may become more complex if intramolecular (e.g. along a conjugated polymer chain) or intermolecular energy transfer is involved.

In case of a spherical molecule there is only one rotational relaxation time ρ which is related to the rotational volume V by the formula (1)

$$\rho = \frac{\eta V}{kT}. \tag{1}$$

For an assymmetric top theory allows up to five different rotational relaxation times to be distinguishable. Symmetric tops with the dipole transition moment parallel to the long axis, however, still exhibit only one rotational relaxation time, and Eq. (1) is applicable in a modified form. (Eq. (4), see below) .

[1] Institut für Physikalische Chemie, Friedrich-Schiller-Universität Jena, Lessingstraße 10, D-07743 Jena, Germany.

[2] To whom correspondence should be addressed; e-mail: ceb@uni-jena.de.

M-C₆C₂: R=2-ethylhexyl   **D**   **P,** n=11
M-C₁₂: R=n-dodecyl

Scheme 1

It is not at all trivial to derive the rotational volume from the molecular dimensions if the molecule bears long conformationally flexible substituents which may not completely follow the rotational diffusion of the emitting chromophore. Scheme 1 shows the chemical structures of just this type of molecule which we have investigated.
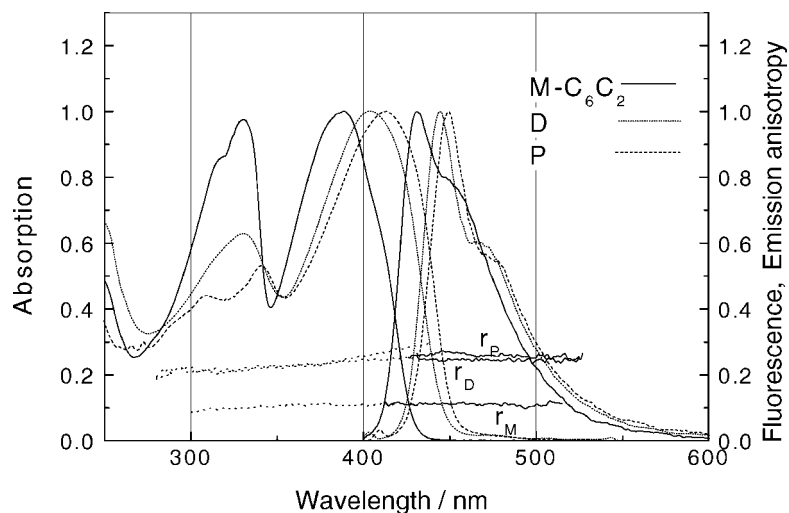
The ellipses depict the rotational volume obtained from the experimental data from Table II. We have found a simplified formula which fits an intuitive imagination of the rotational motion of a prolate symmetric top. At first, however, we shall present some experimental results which categorize compounds M and D as prolate symmetric tops.

RESULTS AND DISCUSSION

Figure 1 contains the normalized absorption and fluorescence spectra and the emission and excitation

Fig. 1. Absorption and fluorescence spectra and emission anisotropy spectra (r_M, r_D, r_P, solid lines) and excitation anisotropy spectra (dotted lines) of M-C_6C_2, D, and P in dioxane.

anisotropy spectra of the compounds M-C_6C_2, D, and P. The spectra and photophysical data of M–C_{12} and M-C_6C_2 are practically identical.

The comparison of the fluorescence spectra of D with P shows that the emitting chromophore in both molecules is nearly the same. Due to their rod-like structure all compounds show a considerable emission anisotropy already in low viscous solvents. Surprisingly, the emission anisotropy of the polymer is only little larger than that of D, in spite of the much larger extension of P (and the shorter fluorescence decay time).

The fluorescence kinetics of all compounds measured with 55° orientation of the analyzer (magic angle) is singly exponential. Figure 2 shows the measured and calculated decay curves of M-C_6C_2.

The fluorescence decay curves measured with vertical ($I_{VV}(t)$) and horizontal ($I_{VH}(t)$) orientation of the second polarizer show a biexponential decay according to the well-known polarized fluorescence kinetics (2).
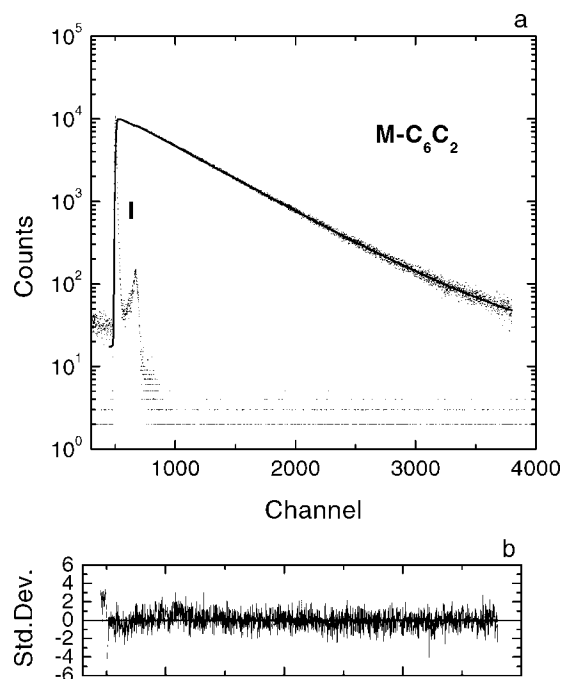
$$I_{VV}(t) = \left(1 + 2r_0 e^{-t/\rho}\right)e^{-t/\tau}$$

$$I_{VH}(t) = \left(1 - r_0 e^{-t/\rho}\right)e^{-t/\tau} \qquad (2)$$

In Fig. 3 the polarized fluorescence decay curves of M-C_6C_2 and P together with the fitted curves are presented. The curves of M-C_6C_2 show the typical decay-decay ($I_{VV}(t)$) and rise-decay ($I_{VH}(t)$) behaviour for the case that the fluorescence decay time τ is larger than the rotational relaxation time ρ.

The biexponential fits $I_{VV(H)} = a_1 \cdot \exp(-t/\tau_1) + a_2 \cdot \exp(-t/\tau_2)$ for M-C_6C_2 results in the following

parameters:

I_{VV}: $a_1 = 0.031$, $\tau_1 = 0.45$ ns, $a_2 = 0.024$,

$\tau_2 = 1.34$ ns, $\chi^2 = 1.08$, Durbin–Watson:1.91;

I_{VH}: $a_1 = -0.031$, $\tau_1 = 0.43$ ns, $a_2 = 0.078$,

$\tau_2 = 1.33$ ns, $\chi^2 = 1.12$, Durbin–Watson:1.79.

Fig. 2. (a) Measured (excitation vertically polarized, emission under magic angle) and calculated decay curves of M-C_6C_2 in dioxane, instrument pulse (I) and (b) residuals. Channel width 2.44 ps.
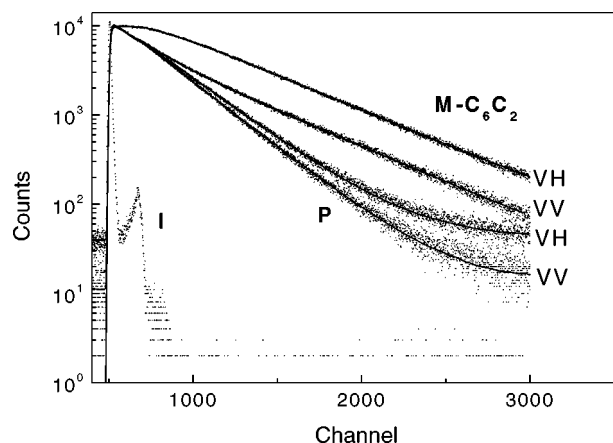
Fig. 3. Excitation pulse (I) and polarized measured (dotted line) and calculated (solid line) decay curves of M-C_6C_2 and P in dioxane. Channel width 2.44 ps.

A different situation is given for the polarized fluorescence kinetics of D and P, where the fluorescence decay time τ is smaller than the rotational relaxation time ρ. In this cases the biexponential fit with free running parameters τ_1 and τ_2 does not lead to physically meaningful results. For the further analysis the model of the Spherical Rotor was used which is implemented in the CD900 software package. This program realizes a global fit procedure which calculates the decay curves I_{VV} and I_{VH} simultaneously. With the fluorescence decay time (determined using magic angle conditions) as a fixed parameter this procedure delivers the rotational relaxation time ρ and the limiting anisotropy r_0.

The results of the stationary and time-resolved fluorescence polarization measurements of the investigated phenyleneethynylene compounds (M-C_6C_2, M–C_{12}, D) and the polyphenyleneethynylene P in dilute solutions at room temperature are given in Table I.

Let us first consider M and D which provide models for the depolarization mechanism without intramolecular energy transfer. The photophysical properties of the M-type compounds (also the spectra) are practically identical. For M and D the emission anisotropies obtained from stationary, r_{stat}, and from time-resolved, r_{kin}, polarization measurements are consistent with each other. The limiting anisotropies r_0 are close to the theoretical value of 0.4. The smaller values of ϕ_f and τ indicate an additional deactivation channel for the polymer P.

In order to obtain a deeper insight into the depolarization mechanism we compare the measured rotational relaxation times with those calculated from the molecular dimensions and the solvent viscosity.

According to their stretched rod-like geometry the molecules can well be described as rotational ellipsoids with a long (a) and a short half-axis (b). The electric dipole transition moment of the longest wavelength absorption is essentially parallel to the long molecular axis as revealed by theoretical calculations with numerous compounds of the same type using time dependent density functional theory (TDDFT) as implemented in the GAUSSIAN-98

Table I. Results of Time-Resolved (Fluorescence Lifetime τ, Limiting Anisotropy r_0, Rotational Relaxation Time ρ) and Steady State (Fluorescence Quantum Yield ϕ_f, Emission Anisotropy r) Polarization Measurements. Solvent Dioxane

	M-$C_6 C_2$	M-C_{12}	D	P
ϕ_f^a	0.90	0.92	0.93	0.77
τ^b	1.34 ns	1.33 ns	0.90 ns	0.76 ns
χ^2	1.18	1.22	1.43	1.19
ρ^c	(0.66 ± 0.01) ns	(0.70 ± 0.01) ns	(2.5 ± 0.5) ns	(6 ± 1) ns
r_0^c	0.38 ± 0.01	0.37 ± 0.01	0.4 ± 0.02	0.36 ± 0.05
χ^{2d}	1.11	1.28	1.49	1.36
DW(I_{VV})	1.88	1.82	1.56	1.58
DW(I_{VH})	1.77	1.68	1.48	1.61
r_{kin}^e	0.125 ± 0.01	0.13 ± 0.01	0.29 ± 0.03	0.32 ± 0.07
r_{stat}^f	0.11 ± 0.01	0.12 ± 0.01	0.25 ± 0.01	0.27 ± 0.01

[a] $\pm 10\%$.
[b] Fluorescence decay times (± 10 ps) and residuals of the fitted decay curve measured with 55° orientation of the second polarizator, from TCSPC-measurements.
[c] Rotational relaxation time and limiting emission anisotropy calculated by the kinetic model of Spherical Rotor Anisotropy (LEVEL2 Analysis package, Edinburgh Analytical Instr.).
[d] Residuals of the Spherical Rotor fit and Durbin–Watson parameters of the calculated curves.
[e] $r_{kin} = r_0/(1 + \tau/\rho)$.
[f] From steady state measurements: $r_{stat} = (I_{VV} - I_{VH})/(I_{VV} + 2I_{VH})$.

package [1] and also by semiempicical methods like CNDO(S) or INDO1(S). For the M-type compound (with the larger alkyl substituents replaced by methyl), for instance, we obtained an angle of 1.3 degrees between the dipole transition moment and the the long molecular axis from TDDFT calculation using the hybrid functional rb3lyp/6-31g(d) after full geometry optimization.

Exclusively rotational motions around axes perpendicular to the long molecular axis contribute to the fluorescence depolarization. Under these conditions the kinetics of the emission anisotropy $r(t)$ is singly exponential with the rotational relaxation time ρ.

$$r(t) = r_0 \cdot e^{-t/\rho} \tag{3}$$

The rotational relaxation time can be calculated according to Navier, Debye, Stokes, Einstein with the help of Eq. (4) [2].

$$\rho = K\left(\frac{a}{b}\right) \cdot C \cdot \rho_S = K\left(\frac{a}{b}\right) \cdot C \cdot \frac{\eta V_S}{kT} \tag{4}$$

with $C = 1$ (stick boundary condition),

$$K\left(\frac{a}{b}\right) = \left[\frac{2}{3} \frac{\left(\frac{a}{b}\right)^4 - 1}{\frac{a}{b}\left[\left(2\left(\frac{a}{b}\right)^2 - 1\right)S - \left(\frac{a}{b}\right)\right]}\right]$$

$$\text{and} \quad S = \frac{\ln\left[\frac{a}{b} + \sqrt{\left(\frac{a}{b}\right)^2 - 1}\right]}{\sqrt{\left(\frac{a}{b}\right)^2 - 1}},$$

where $K(a/b)$ accounts for deviations from spherical symmetry, and V_s is the volume of the rod like molecule approximated as rotational ellipsoid.

Figure 4 shows the correction factor $K(a/b) = \rho/\rho_S$ as a function of the axial ratio a/b.

Obviously, ρ/ρ_S is approximately equal to the axial ratio a/b itself in the region $1 < a/b < 8$. Under these circumstances Eq. (4) is simplified to Eq. (5) and the volume $V = 4/3\pi a^2 b$ becomes the rotational volume.

$$\rho \approx \rho_S \cdot \frac{a}{b} = \frac{\eta}{kT} \cdot V_S \cdot \frac{a}{b}$$

$$= \frac{\eta}{kT} \cdot \frac{4\pi}{3} ab^2 \cdot \frac{a}{b} = \frac{\eta}{kT} \cdot \frac{4\pi}{3} a^2 b \tag{5}$$

In order to calculate the rotational relaxation times of the compounds investigated we have determined the corresponding half axes of the ellipsoids from the molecular geometry. Taking into account the conformational flexibility of the alkoxy side chains we have varied the length of the short half axis from $b = 218$ pm (side chain bent parallel to long axis or without side chain at all) to fully stretched side chains. In another way, the short half axis was directly calculated from the measured rotational re-
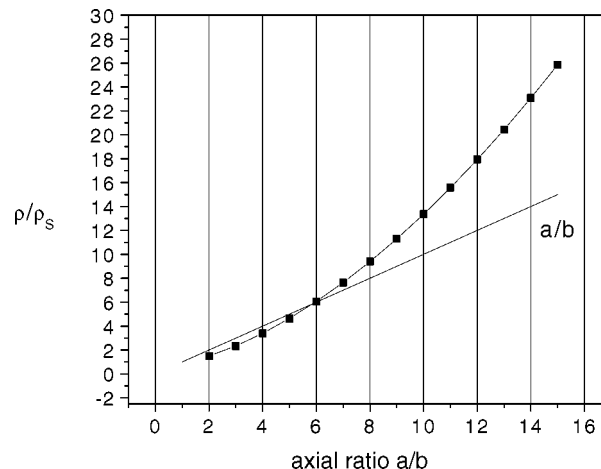
Fig. 4. Ratio of the rotational relaxation times $\rho/\rho_S = K(a/b)$ versus a/b (Eq. 4).

laxation time and the rotational volume using Eq. (5). The results are compiled in Table II.

Table II shows that for M and D the experimental values of ρ and b_ρ are near the lower theoretical limits. The M-type compounds exhibit emission anisotropies and rotational relaxation times almost independent of the length of the side chains, that is, the side chains do not contribute to the rotational volume. Fluorescence depolarization occurs through rotational motion perpendicularly to the long molecular axis around an axle which contains the side chains.

The same depolarization mechanism occurs with D. However, the short half axis b_ρ determined from the experimental data with (3) is enlarged in comparison with M. The side chains of D cannot coincide with the axle of revolution and do contribute to the rotational volume.

Included in Scheme 1 are the rotational ellipsoids for M-C_6C_2 and D with the half axes a and b_ρ corresponding with the data in Table II.

Table II. Calculated Rotational Relaxation Times and Short half axes. Solvent Dioxane ($T = 293$ K, $\eta = 1.26$ cP)

	M-C_6C_2	M-C_{12}	D	P
a/pm	1350	1350	2240	10000
b/pm	218–970	218–1565	218–1030	218–1910
a/b	6.19–1.39	6.19–0.86	10.28–2.17	45.9–5.24
ρ_c/ns[a]	0.53–1.89	0.52–3.35[d]	1.94–5.07	108–237
ρ/ns[b]	0.66 ± 0.01	0.70 ± 0.01	2.5 ± 0.5	6 ± 1
b_ρ/pm[c]	277 ± 4	292 ± 4	383 ± 80	„38 ± 6"

[a] According Eq. (2).
[b] Experimental values from Table I.
[c] Short half axes according Eq. (3): $b_\rho = (3kT\rho)/4\pi\eta a^2$.
[d] $S(a/b < 1) = (1 - (a/b)^2)^{-1/2} \tan^{-1}[(1-(a/b)^2)^{1/2})/(a/b)]$, according [2], p. 130.

The rotational relaxation times of M and D calculated from a simple model agree well with the experimental ones. For compounds with these dimensions the calculation of the rotational relaxation times from the simple model according Eq. (5) is a good approximation.

The situation is different with P. The calculated rotational relaxation time Eq. (3) with more than 100 ns is far from the experimentally determined one and the calculated short molecule axis b_ρ (Eq. (5)) is unrealistically small. Obviously, fluorescence depolarization cannot be determined by rotational motion perpendicularly to the long molecular axis. Nevertheless, both the decrease of the steady state anisotropy r_{stat} in comparison with r_0 as well as the experimentally determined rotational relaxation time of 6 ns indicate an effective depolarization mechanism in which molecular motions take part. In order to interpret the experimental findings one has to take into consideration that the polymer molecules do not adopt their idealized linear stretched geometry rather than exist as a distribution of differently bent conformations in a dynamical equilibrium. Thus, since the excitation energy is located to very few repetion units of the polymer chain [3], even poorly efficient migration gives rise to depolarization.

EXPERIMENTAL

The synthesis of the compounds M-C_6 C_2 and D have been described in [4], the synthesis of compound M-C_{12} in [5] and the synthesis of the polymer P in [3].

Corrected fluorescence spectra and the fluorescence polarization were measured using a LS50B luminescence spectrometer (Perkin Elmer). Fluorescence quantum yields were determined relative to quinine sulphate (purum; FLUKA) in 0.1 N H_2SO_4 with $\Phi_f = 0.55$ used as a standard.

Picosecond time-resolved fluorescence polarization experiments were performed with an OB900 Fluorescence Lifetime Spectrometer (Edinburgh Analytical Instruments) using a frequency doubled mode locked titanium–sapphire laser (100 fs, 104 MHz, 400 nm, 1 nJ/pulse) as the excitation source and a Hamamatsu microchannel plate photomultiplier (MCP-PMT R3809U-50 and a SPC-430 single photon counting board (Becker & Hickl, Berlin) as the detection unit. Glan–Tompson prisms inserted between the monochromators and the sample compartment were used as polarizers. The width of the instrument pulse is 35 ps due to the rise time of the photomultiplier. In order to calculate the fluorescence lifetime, the LEVEL 1 (up to 4 exponentials) and LEVEL 2 (Spherical Rotor) packages implemented in the Edinburgh Analytical Instruments software were used. The analysis makes use of the iterative reconvolution technique and the Marquardt fitting algorithm. The Spherical Rotor program is a global fitting procedure for the determination of the parameters τ, ρ and r_0 using the $I_{VV}(t)$ and $I_{VH}(t)$ decay curves according Eq. (2). Further details are given in [3].

REFERENCES

1. Gaussian 98, Revision A.11.4, M. J. Frisch, G. W. Trucks, H. B. Schlegel, G. E. Scuseria, M. A. Robb, J. R. Cheeseman, V. G. Zakrzewski, J. A. Montgomery, Jr., R. E. Stratmann, J. C. Burant, S. Dapprich, J. M. Millam, A. D. Daniels, K. N. Kudin, M. C. Strain, O. Farkas, J. Tomasi, V. Barone, M. Cossi, R. Cammi, B. Mennucci, C. Pomelli, C. Adamo, S. Clifford, J. Ochterski, G. A. Petersson, P. Y. Ayala, Q. Cui, K. Morokuma, N. Rega, P. Salvador, J. J. Dannenberg, D. K. Malick, A. D. Rabuck, K. Raghavachari, J. B. Foresman, J. Cioslowski, J. V. Ortiz, A. G. Baboul, B. B. Stefanov, G. Liu, A. Liashenko, P. Piskorz, I. Komaromi, R. Gomperts, R. L. Martin, D. J. Fox, T. Keith, M. A. Al-Laham, C. Y. Peng, A. Nanayakkara, M. Challacombe, P. M. W. Gill, B. Johnson, W. Chen, M. W. Wong, J. L. Andres, C. Gonzalez, M. Head-Gordon, E. S. Replogle, and J. A. Pople, Gaussian, Inc., Pittsburgh PA, 2002.
2. G. R. Fleming (1986). *Chemical Applications of Ultrafast Spectroscopy, International Series of Monographs on Chemistry*, Vol. 13. Oxford University Press, Clarendon Press, Oxford, New York, pp. 124–133.
3. U.-W. Grummt, Th. Pautzsch, E. Birckner, H. Sauerbrey, A. Utterodt, U. Neugebauer, and E. Klemm (2004). Photophysics of poly[2,2′-bipyridine-5,5′ diylethynylene-(2,5)-di(2-ethylhexyl)oxy-1,4-phenylene)ethynylene]. A comparison with monomer and dimer model compounds. *J. Phys. Org. Chem.* **17**, 1–8.
4. T. Pautzsch and E. Klemm (2002). Ruthenium-chelating poly(heteroarylene-ethynylene)s: Synthesis and properties. *Macromolecules* **35**, 1569–1575.
5. U.-W. Grummt, E. Birckner, E. Klemm, D. A. M. Egbe, and B. Heise (2000). Conjugated polymers with 2,2′-bipyridine and diethinylenebenzene units: Absorption and luminescence properties. *J. Phys. Org. Chem.* **13**, 112–126.